Corrosion Science 110 (2016) 296–304

Contents lists available at ScienceDirect

Corrosion Science

journal homepage: www.elsevier.com/locate/corsci

Sustained effect of remaining cementite on the corrosion behavior of ferrite-pearlite steel under the simulated bottom plate environment of cargo oil tank

Xuehui Hao, Junhua Dong*, Ini-Ibehe Nabuk Etim, Jie Wei, Wei Ke

State Key Laboratory for Corrosion and Protection, Institute of Metal Research, Chinese Academy of Sciences, Shenyang 110016, China

ARTICLE INFO

Article history:
Received 17 March 2016
Received in revised form 24 April 2016
Accepted 26 April 2016
Available online 28 April 2016

Keywords:
A. Steel
A. Acid solutions
B. SEM
B. Polarization
B. EIS

ABSTRACT

This investigation aims to study the sustained effect of remaining cementite on the corrosion of ferrite-pearlite steel in an acidic chloride solution (i.e. simulated bottom plate environment of cargo oil tank). The results show that the corrosion rate of ferrite-pearlite steel was continuously accelerated with extending the immersion time, caused by the continuously enhanced galvanic effect between the remaining lamellar cementite and exposed ferrite phases. Electrochemical impedance spectroscopy (EIS) data further indicated that the promoted dissolution of ferrite phases was controlled by charge transfer process. Meanwhile, the hydrogen evolution reaction occurred on cementite was controlled by the diffusion process.

1. Introduction

Ferrite-pearlite steels are widely used in engineering fields, such as infrastructures, shipping, mechanical equipment and so forth, where high strength, wear resistance, ductility, toughness, and low cost are of immense importance [1–4]. Generally, pearlite has a typical lamellar structure consisting of alternating layers of ferrite and cementite (Fe_3C) [5]. It is well-known that although Fe_3C can improve the mechanical properties [6–9], its existence is harmful to the corrosion resistance of steels. Staicopolus [10,11] reported that cementite with a low hydrogen over-voltage would act as cathodic sites to promote the corrosion of ferrite phase of the steel in an acidic solution. Moreover, since the ferrite phase dissolved preferentially as anode and the cementite was insoluble as cathode, it could be inferred that the area of exposed cementite increased gradually and even a covering porous layer was formed on the surface, which caused a continuous acceleration in the anodic dissolution rate during the corrosion evolution process [12]. Certainly, this kind of corrosion was widely found in other conditions such as the dezincification of brass [13–15], the preferential dissolution of α phase in AZ91 magnesium alloy [16–18], crevice corrosion in bolt screw fixing system [19], and corrosion under deposit [20]. Several other studies revealed that the corrosion rate of steels was enhanced by the increasing volume fraction of cementite phases [21–25]. However, cementite phases could also have the beneficial effect on corrosion resistance of steels because they could promote the precipitation of a well adhered corrosion product [26–29]. Furthermore, it was reported that the localized corrosion rate of cargo oil tank bottom of a very large crude carrier (VLCC) could reach a maximum depth reduction of about 4 mm/y [30–32]. The main reason is that the salt concentration in crude oil contained salt water is several times higher than that in seawater. Moreover, this salt water could be separated from crude oil and accumulate on the bottom of tanks inducing the corrosion pits on the inner surface of tanks. Subsequently, the growth of corrosion pits could cause the penetration of tanks and finally result in oil leaking. The International Maritime Organization (IMO) [33] has suggested that the accumulated salt water inside the pits could be specified by an acidic chloride solution containing 10 wt.% NaCl with pH = 0.85. For the uniform corrosion of ferrite-pearlite steels in this medium, it may be inferred that Fe_3C as the cathode will accumulate continuously on the surface after the preferential dissolution of ferrite, which may enhance galvanic corrosion. To authors' best of knowledge, no research report has studied the sustained effect of remaining Fe_3C on the corrosion of ferrite-pearlite steel in an acidic chloride solution simulating the bottom plate environment of cargo oil tank.

In this work, the target is to deeply disclose the continuously enhanced galvanic effect of the remaining Fe_3C caused by the pref-

---

* Corresponding author.
E-mail address: jhdong@imr.ac.cn (J. Dong).

http://dx.doi.org/10.1016/j.corsci.2016.04.042

erential dissolution of ferrite phase on the corrosion evolution of ferrite-pearlite steel investigated by gravimetric tests, scanning electron microscope (SEM), X-ray diffraction (XRD), electrochemical polarization technique and electrochemical impedance spectroscopy (EIS).

2. Experimental

Ferrite-pearlite steel composed of the following elements (wt.%) of 0.35C, 0.25 Si, 0.56 Mn, 0.016 P, 0.003 S and Fe (balance) was used in this investigation. Samples with dimensions of 60 mm × 25 mm × 5 mm were prepared for immersion test and samples with dimensions of 10 mm × 10 mm × 5 mm were prepared for electrochemical measurements, respectively. The sample was mechanically ground with SiC paper from 80 to 1000 grit, rinsed with deionized water and degreased with absolute ethanol. After being dried with cold air, the pre-weighted samples were completely immersed in the acidic chloride solution of 10 wt.% NaCl with pH = 0.85 (adjusted with hydrochloric acid) at 30 ± 2 °C for 24, 48, 72, 144 and 216 h, respectively. Three parallel samples of the ferrite-pearlite steel were tested in the same condition and test solution was changed to new one every 24 h to minimize pH change of the test solution. For the weight loss measurement, corroded samples were immersed in the cleaning solution containing 20% HCl and 2% Hexamethylenetetramine ($C_6H_{12}N_4$) and stirred for about 10 min at 25 °C, which was in accordance with ASTM G1-03 standard [34]. Then the samples were rinsed with deionized water and absolute ethanol, dried and reweighed. The thickness loss and the average corrosion rate of the ferrite-pearlite steel in the acidic chloride solution were calculated based on the following equations:

$$X = \frac{\Delta W}{\rho S} \times 10000 \tag{1}$$

$$\nu = \frac{\Delta W}{\rho S t} \times 10 \times 365 \times 24 \tag{2}$$

where X is the thickness loss of the ferrite-pearlite steel (μm), n the average corrosion rate of the ferrite-pearlite steel (mm/y), ΔW the weight loss of the ferrite-pearlite steel (g), ρ the density of the tested steel ($\mathrm{g\,cm^{-3}}$), S the total surface area of the sample ($\mathrm{cm^2}$), t the immersion time (h). In this study, ρ is regarded as $7.8\ \mathrm{g\,cm^{-3}}$.

A Canon camera (A620), a Zeiss light optical microscope (Axio Cam MRc 5, OM) and a FEI scanning electron microscopy (Inspect$^{\mathrm{TM}}$ F, SEM) were employed to observe the surface morphologies of the samples after immersion for 0 and 216 h. The exposed sample used for microstructure analysis was ground, mechanically polished with diamond paste of 2.5 μm particle size, and then etched with 4 vol.% nitric acid in absolute ethanol. For the cross-sectional SEM observation, the corroded sample was encapsulated in epoxy resin, cut into the size of 15 mm × 25 mm × 5 mm, and finally polished in absolute ethanol with diamond paste of 2.5 μm particle size.

A Rigaku-D/max 2000 X-ray diffraction (Shimadzu XD-5A, XRD) employing Cu Ka radiation source was used to analyze the phase composition of the samples after immersion for 0 and 216 h. The XRD spectra were recorded in 2θ values of 10–85 under 50 kV and 250 mA at a scanning rate of 2/min.

A Gmary DC105 electrochemical workstation using a conventional three electrodes cell was employed to perform electrochemical measurements, where a platinum plate was used as the counter electrode, a saturated calomel electrode (SCE) as the reference electrode, and the sample made of the ferrite-pearlite steel with an exposed area of 1 $\mathrm{cm^2}$ as the working electrode. The working electrode was immersed in the acidic chloride solution for 0, 24, 48, 72, 144 and 216 h, separately. Then, the potentiodynamic polarization tests and electrochemical impedance spectroscopy (EIS) measurements were carried out. The polarization curves were obtained by polarizing in the range between −250 and +250 mV with respect to the open circuit potential (OCP) at a 10 mV/min scan rate. EIS was measured over the frequency range of 100 kHz–10 mHz with a 10 mV amplitude signal at OCP. The OCP of samples during the immersion test was monitored by a HA-151A potentiostat. Each electrochemical test was conducted at least twice for repeatability. All of the potentials are with respect to SCE.

3. Results and discussion

3.1. Surface analysis

Fig. 1(a) shows the metallographic photo of the exposed ferrite-pearlite steel. It can be seen that the microstructure is composed of granular ferrite phase (white area) and pearlite phase (black area). The ferrite phase appears as several irregular shapes such as strips and lumps. Meanwhile, their grain sizes are not uniform. However, the pearlite phase appears as big lumps. Based on the intercept method [35], the average grain size is measured to be about 30 μm. Additionally, the area fraction of pearlite on the steel surface measured by quantitatively metallographic is about 54%. Fig. 1(b) presents the SEM image of the exposed ferrite-pearlite steel. It shows that pearlite is a lamellar structure and composed of alternating layers of ferrite and cementite (Fe_3C), while ferrite phases appeared as a uniformed appearance.

Fig. 2(a and b) shows the macro-morphologies of the ferrite-pearlite steel after immersion for 0 and 216 h in the acidic chloride solution, respectively. Fig. 2(a) illustrates that the exposed steel surface is smooth and exhibits grey color. Comparing Fig. 2(b) with (a), a thin and black layer was formed on the surface after the steel was immersed for 216 h. The micro-morphologies corresponding to optical photos are shown in Fig. 2(a′ and b′), respectively.

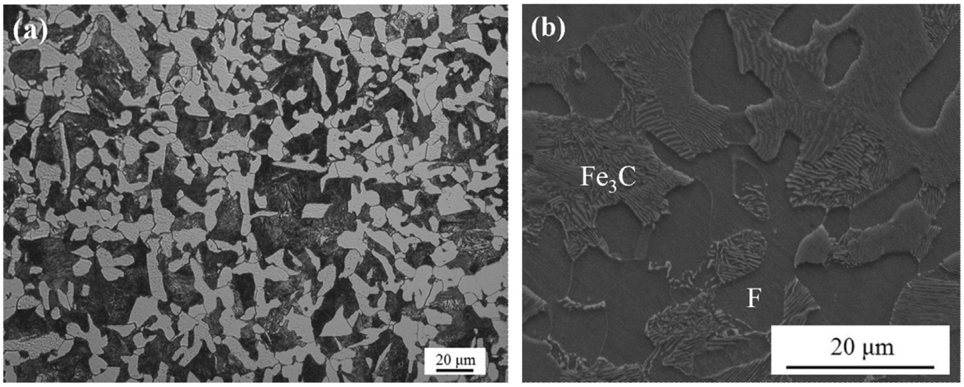

Fig. 1. The microstructure of the exposed ferrite-pearlite steel (a) metallographic photo; (b) SEM image;.